

## Unravelling the mechanical behaviour of advanced multiphase steels isothermally obtained below $M_s$

Navarro-López, Alfonso; Hidalgo, Javier; Sietsma, Jilt; Santofimia, Maria J.

**DOI**

[10.1016/j.matdes.2020.108484](https://doi.org/10.1016/j.matdes.2020.108484)

**Publication date**

2020

**Document Version**

Final published version

**Published in**

Materials and Design

**Citation (APA)**

Navarro-López, A., Hidalgo, J., Sietsma, J., & Santofimia, M. J. (2020). Unravelling the mechanical behaviour of advanced multiphase steels isothermally obtained below  $M_s$ . *Materials and Design*, 188, Article 108484. <https://doi.org/10.1016/j.matdes.2020.108484>

**Important note**

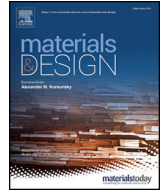
To cite this publication, please use the final published version (if applicable). Please check the document version above.

**Copyright**

Other than for strictly personal use, it is not permitted to download, forward or distribute the text or part of it, without the consent of the author(s) and/or copyright holder(s), unless the work is under an open content license such as Creative Commons.

**Takedown policy**

Please contact us and provide details if you believe this document breaches copyrights. We will remove access to the work immediately and investigate your claim.



# Unravelling the mechanical behaviour of advanced multiphase steels isothermally obtained below $M_s$

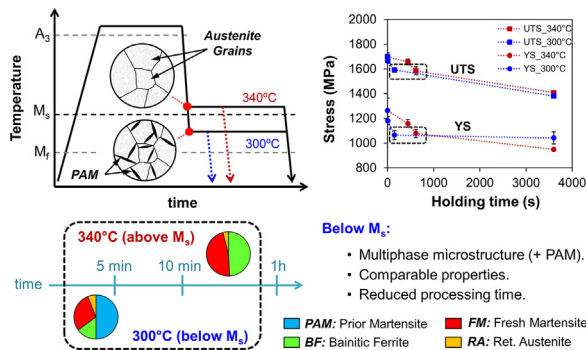
Alfonso Navarro-López\*, Javier Hidalgo, Jilt Sietsma, Maria J. Santofimia

Department of Materials Science and Engineering, Delft University of Technology, Mekelweg 2, 2628 CD Delft, the Netherlands

## HIGHLIGHTS

- Holding time effect on microstructure-properties relationship of a low-C steel isothermally treated below  $M_s$  is discussed.
- The mechanical behaviour of below- $M_s$  multiphase steels is primarily affected by the distinct tempering degree of martensite.
- The bainitic character of the isothermal product phase formed below  $M_s$  is confirmed by the analysis of Kocks-Mecking plots.
- Multiphase steels obtained below  $M_s$  exhibit comparable properties to conventional steels after shorter processing routes.

## GRAPHICAL ABSTRACT



## ARTICLE INFO

### Article history:

Received 30 October 2019  
 Received in revised form 3 January 2020  
 Accepted 8 January 2020  
 Available online xxxx

### Keywords:

Multiphase steels  
 Microstructure-properties  
 Prior athermal martensite  
 Tempering  
 Bainite formation  
 Yielding behaviour

## ABSTRACT

The initial formation of athermal martensite was proven to accelerate the subsequent bainite formation kinetics during isothermal holdings below the martensite-start temperature ( $M_s$ ). The presence of prior athermal martensite (PAM) within the phase mixture is expected to modify the overall mechanical response of these newly-designed multiphase steels. Differences stem not only from the balance of product phases, but also from the effect of tempering of the PAM with variations in the applied holding time. This work investigates the effect of tempering time on the mechanical behaviour of the PAM and, as consequence, on the overall mechanical response of these microstructures. Results show that, for short holding times (several minutes), PAM yields similar to as-quenched martensite while, for longer holding times, its yielding behaviour becomes comparable to the one exhibited by typical tempered martensite. Furthermore, the use of Kocks-Mecking curves for the analysis of the mechanical performance confirms the bainitic character of the product phase isothermally formed below  $M_s$ . Tailoring the bainitic-martensitic microstructure with variations of the holding time below  $M_s$  enables to obtain advanced multiphase steels with comparable mechanical properties to those exhibited by conventional bainitic steels, but in shorter processing times due to the acceleration of bainite formation.

© 2020 The Author(s). Published by Elsevier Ltd. This is an open access article under the CC BY-NC-ND license (<http://creativecommons.org/licenses/by-nc-nd/4.0/>).

## 1. Introduction

A new metallurgical route has been recently proposed for the manufacturing of new advanced high strength steels (AHSS) through a more promising sustainable processing route which could lead to a

\* Corresponding author.  
 E-mail address: [a.navarrolopez@tudelft.nl](mailto:a.navarrolopez@tudelft.nl) (A. Navarro-López).

reduction in production time and energy consumption, and, as a consequence, in reduced greenhouse gas emissions. The novelty of this new metallurgical route lies on the acceleration of the bainite reaction through the presence of athermal martensite previously formed during the thermal cycle [1–6]. This thermal cycle consists of a fast cooling from full austenitization to an intermediate temperature between the martensite-start ( $M_s$ ) and martensite-finish ( $M_f$ ) temperatures, followed by an isothermal holding below  $M_s$  and a final cooling to room temperature. During the initial interrupted cooling, a certain fraction of prior athermal martensite (PAM) is formed before the bainite reaction occurring in the subsequent holding below  $M_s$  [6–10]. The formation of PAM implies the introduction of martensite-austenite interfaces which, in addition to prior austenite grain boundaries, act as preferential nucleation sites for bainite nucleation [3,6]. The presence of these newly-formed interfaces drastically increases the number of potential nucleation sites and, as consequence, leads to an acceleration by several orders of magnitude of the bainite formation in comparison with the one that takes place without the presence of PAM [6]. The final fraction of bainitic ferrite (BF) formed depends on the isothermal holding temperature and time, respectively. However, the bainite reaction often remains incomplete and a certain fraction of austenite still remains untransformed after the formation of PAM and BF. The remaining fraction of untransformed austenite is either transformed into fresh martensite or retained after the final cooling to room temperature. As a result, the final multiphase microstructure contains a martensitic-bainitic matrix in combination with martensite-austenite (MA) islands as well as carbon-enriched austenite.

Recent investigations on low-carbon steels, alloyed with medium-manganese and/or high-silicon contents, heat treated through the proposed thermal cycles show that a good combination of mechanical properties can be attained, similar, in many cases, to the ones exhibited by conventional bainitic steels [5,11–18]. The main difference between both types of microstructures lies in the presence of PAM in those isothermal holdings below  $M_s$ . The formation of PAM affects the overall mechanical response of these multiphase steels. First, PAM can contribute, in principle, to the strengthening of the phase mixture since it is initially a carbon-supersaturated martensitic phase. Secondly, the fragmentation of the initial austenite grains due to the formation of PAM favours the increase of the yield stress through the reduction of the average bainite sheaf size [5,18]. Finally, the tempering of PAM with holding time leads to the softening of this micro-constituent due to the precipitation of carbon in solid solution in the form of carbides as well as dislocations recovery, affecting both phenomena the mechanical behaviour of the steel.

Variation of the holding time gives rise to different degrees of tempering of the PAM, resulting in different individual mechanical response of this product phase within the final phase mixture. The tempering process can be divided into several stages, arranged in order of increasing tempering temperature. At low temperatures, carbon atoms segregate at dislocations, phenomenon that can occur even during quenching. At intermediate temperatures, transitional carbides start to precipitate within the martensitic matrix. Finally, at highest temperatures of the tempering range, transitional carbides transform into cementite, which coarsens upon extended tempering times [19]. All these phenomena lead to the softening of the PAM due to changes in its matrix, which can be aggravated by the recovery of dislocations from intermediate holding temperatures (generally, higher than approximately 400 °C). Previous investigations on this type of multiphase steels show that the presence of PAM leads to an increase of the yield stress together with a reduction of the tensile strength in specimens annealed below  $M_s$  in comparison to those isothermally treated above  $M_s$  [5,11,14,15,17,18]. Among these investigations, only a few research studies show the evolution of the mechanical properties of specimens isothermally treated below  $M_s$  at different holding times [14,17]. These studies report a rapid decrease of the yield stress at short holding times (only a few minutes) and, then, an increase of the yield stress with

longer holding times. On the contrary, a decreasing evolution of the ultimate tensile strength is reported with respect to the increasing holding time.

A deeper analysis of the evolution of the mechanical properties is still needed by taking into consideration all product phases formed in these advanced multiphase steels. This will allow to understand the effect of holding time not only on the degree of tempering of PAM and its individual mechanical behaviour, but also on the microstructure-properties relationship derived from the multiphase mixture formed in which bainitic ferrite and/or retained austenite are also present. This research work investigates the mechanical behaviour of prior athermal martensite after the application of different holding times below  $M_s$  and, consequently, its effect on the formation of other phases and on the overall mechanical behaviour of these multiphase steels. The evolution of the microstructure and the resulting properties are studied by the application of different isothermal treatments above and below  $M_s$  in a low-carbon steel. The resulting properties are compared and benchmarked against the mechanical properties reported in other research studies as well as other conventional grades of advanced high strength steels.

## 2. Experimental procedure

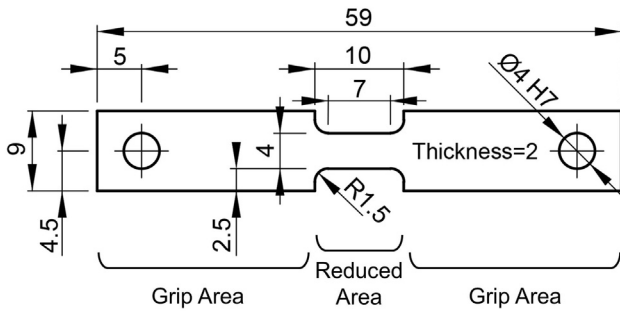
The chemical composition of the alloyed steel investigated in the present work is indicated in Table 1. Double T-shaped tensile specimens and cylindrical dilatometry specimens were machined parallel to the rolling direction of a hot rolled slab of 4 mm thickness. The dimensions of these specimens are indicated in Fig. 1. All specimens were extracted from the same steel slab used in previous works of the present authors [6,20], but from a different slab area. Local compositional variations of the hot rolled slab led to slight differences in the critical temperatures of the steel, such as the  $M_s$  temperature, compared to those reported in [6,20]. A Bähr 805A/D dilatometer was primarily used to thermally treat all specimens and, secondarily, to identify phase transformations occurring during the applied heat treatments. All specimens were inductively heated up under vacuum conditions of the order of  $10^{-4}$  mbar and cooled down under a protective atmosphere of continuously-flushed helium gas. An S-type thermocouple was spot-welded on the surface of each specimen to control and monitor the temperature at any instant.

Fig. 2 shows a schematic overview of the heat treatments applied to both types of specimens. Three tensile specimens were used per each thermal condition to obtain a statistical representativeness of their mechanical performance under tensile deformation. On the other hand, only one dilatometry specimen was used per thermal condition to identify the phase transformations occurring during each heat treatment. A direct-quench from full austenitization to room temperature was carried out to determine the mechanical response of a fully untempered martensitic microstructure. The experimental  $M_s$  temperature was determined at  $M_s(1\%) = 335 \text{ °C} \pm 5 \text{ °C}$  [18]. Three isothermal treatments with different holding times ('t1', 't2', 't3', see Table 2) after full austenitization were performed at each of the three selected temperatures to obtain intermediate fractions of bainitic ferrite and determine the mechanical response of the resulting microstructures. The phase fractions formed after each heat treatment were determined from the dimensional changes detected by dilatometry of the heat-treated cylindrical specimens. Experimental results derived from isothermal treatments 't3' at the three selected temperatures were previously analysed in detail elsewhere [18].

**Table 1**  
Chemical composition (in wt. pct) of the alloyed steel with balanced iron (Fe).

| C    | Mn   | Si   | Mo   | Al   |
|------|------|------|------|------|
| 0.20 | 3.51 | 1.52 | 0.25 | 0.04 |

(a) T-shaped tensile specimen:



(b) Cylindrical dilatometry specimen:

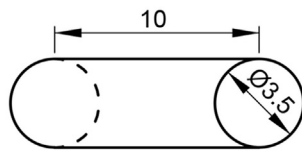


Fig. 1. Schematic representation of tensile and cylindrical specimens with their dimensions in mm.

An Instron 5500R electromechanical tester machine was used to perform all tensile tests, which were carried out in extension control at room temperature. A clip-on extensometer with knife edges was used to measure the elongation of the specimen gauge during the tensile test. The attachment of the extensometer to the tensile specimen consisted of fixing firmly by elastic bands the knife edges of the extensometer in both extremes of the specimen gauge. The extensometer, with a separation between knife edges of 7.8 mm, completely covered the gauge length of the double T-shaped specimen. Once tensile tests were performed, mechanical properties such as yield stress, tensile strength, and uniform elongation were determined from the corresponding engineering stress-strain curves of all heat treated specimens. In this work, the 0.2% offset method was used for the determination of the yield stress ( $\sigma_y$ ).

Cross sections of heat-treated cylindrical specimens were grinded and polished to 1  $\mu\text{m}$ , and etched with 2% Nital to observe the microstructures obtained after heat treatments. A JEOL JSM-6500F Scanning Electron Microscope (SEM) was used for the microstructural characterization, using a 15 kV electron beam and the Secondary Electron Imaging (SEI) detection mode. A Bruker D8-Advance diffractometer was used to perform X-ray diffraction (XRD) measurements in order to

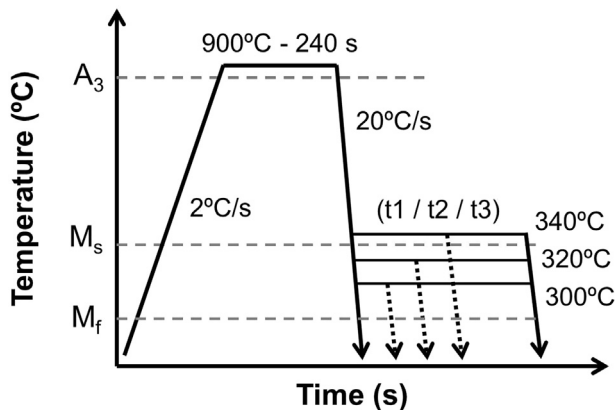


Fig. 2. Direct-quench and isothermal treatments ( $t_1/t_2/t_3$ ) performed to both types of specimens.

Table 2

Holding times ( $t_1$ ,  $t_2$ ,  $t_3$ ) applied during the isothermal stage performed at the three selected temperatures.

| HT    | Isothermal holding time (s) |        |        |
|-------|-----------------------------|--------|--------|
|       | 300 °C                      | 320 °C | 340 °C |
| $t_1$ | 7                           | 253    | 441    |
| $t_2$ | 151                         | 422    | 615    |
| $t_3$ | 3600                        | 3600   | 3600   |

determine the retained austenite fraction in the cylindrical specimens. These measurements were carried out by using Co-K $\alpha$  radiation. A 2 $\theta$  scan from 40° to 130° was performed in all specimens with a step size of 0.035°. The integrated area method was used to calculate the fractions of retained austenite by comparing the areas under the {200}, {220}, and {311} diffraction peaks of fcc-austenite with the areas under the {110}, {200}, {211}, and {220} diffraction peaks of the bcc-phase(s) [21].

### 3. Results

#### 3.1. Formation of product phases

Dilatometry curves for cylindrical specimens isothermally treated at 340 °C, 320 °C, and 300 °C for holding times  $t_1$ ,  $t_2$ , and  $t_3$  are shown in Fig. 3a-c. All specimens exhibit a linear behaviour during cooling from austenitization until reaching the  $M_s$  temperature. This is an indication of the non-decomposition of austenite into bcc-phases, such as ferrite, pearlite, or bainite, before the onset of the austenite-to-martensite transformation. In treatments performed at 340 °C (above  $M_s$ ), there is a length increase (dilatation) in all specimens during the isothermal holding which is originated by the formation of bainitic ferrite (BF) (see Fig. 3a). In treatments performed at 320 °C and 300 °C (below  $M_s$ ), a deviation from linearity occurs once the  $M_s$  temperature is overcome during cooling due to the formation of prior athermal martensite (PAM), as indicated in Fig. 3b-c.

The austenite-to-martensite transformation stops when the cooling is interrupted at the corresponding isothermal temperature. Subsequently, dilatation takes place during all isothermal holdings as consequence of the formation of bainitic ferrite (see Fig. 3b-c).

Finally, there is a deviation from linearity of the change in length during the final cooling from the isothermal temperatures to room temperature in all experimental dilatometric curves, as shown in Fig. 3a-c. This deviation is an indicative of the decomposition of untransformed austenite into fresh martensite (FM). In all cases, the isothermal bainitic transformation is incomplete even after 1 h of holding time and the remaining untransformed austenite partially transforms into fresh martensite, while the rest is partially retained at room temperature.

The quantification of the phase fractions was first performed in the one-hour isothermal treatments ( $t_3$ ). In these heat treatments, the volume fractions of fresh martensite, originated from the untransformed austenite decomposition during the final cooling, were obtained from the dilatometry data by following the procedure described in ref. [6]. The bainitic ferrite fractions were balanced from volume fractions of the rest of product phases, i.e., from prior athermal martensite, fresh martensite (both obtained from dilatometry), and retained austenite (obtained from XRD). For the isothermal treatments  $t_1$  and  $t_2$ , bainitic ferrite fractions were extracted from the dilatometry curves of the one-hour isothermal treatments ( $t_3$ ) by considering the fraction formed at the selected holding times for each of the three temperatures (see Table 2). In these heat treatments, the fresh martensite fractions were balanced from the volume fractions of prior athermal martensite, bainitic ferrite (both obtained from dilatometry), and retained austenite (obtained from XRD).

Fig. 4a-c show the evolution of the volume fractions of the distinct phases of the multiphase mixture formed after the application of the

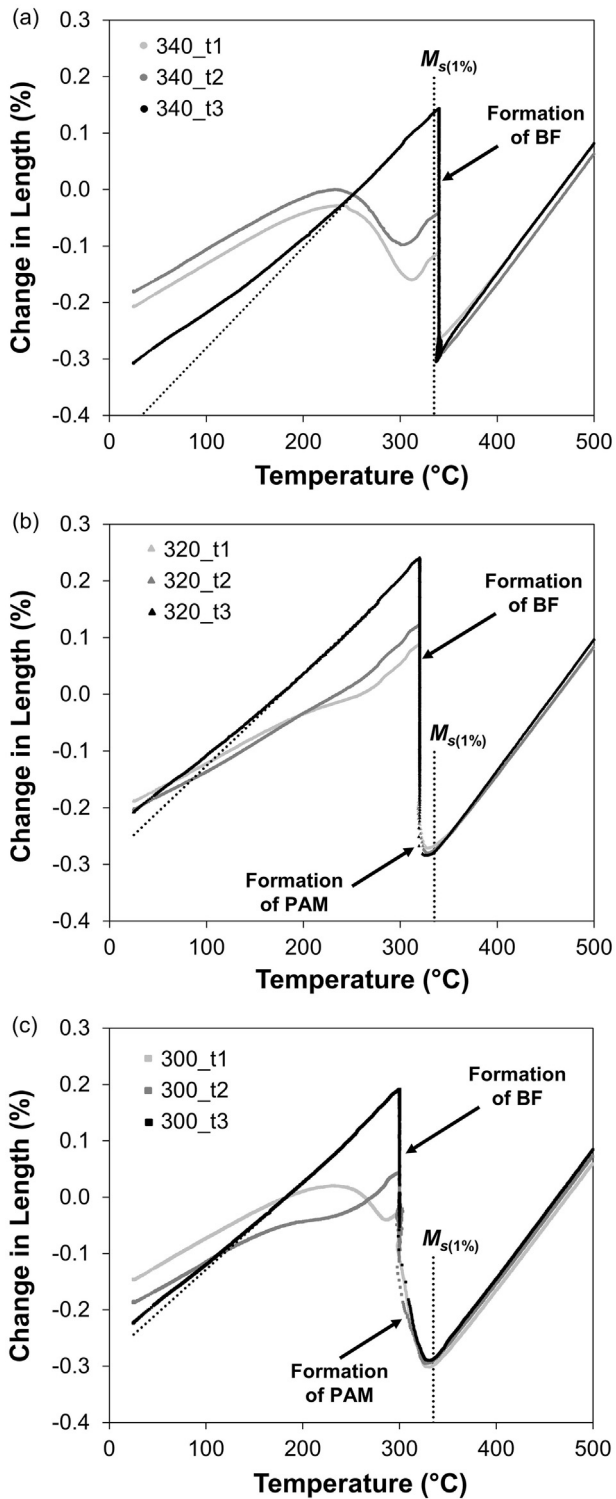


Fig. 3. Change in length of cylindrical dilatometry specimens during cooling stages and isothermal holdings at (a) 340 °C, (b) 320 °C, and (c) 300 °C for different holding times (t1, t2, and t3). The experimental  $M_s$  temperature is also shown.

previously described isothermal treatments at 340 °C, 320 °C, and 300 °C, respectively. Implicitly, the final balance of phase fractions for each thermal-temporal condition can be extracted from these figures. As is observed, the volume fraction of PAM is maintained constant with holding time at each temperature since it only depends on the undercooling below  $M_s$ . The volume fraction of bainitic ferrite increases with holding time at all temperatures and, as consequence, a lower volume fraction of fresh martensite is formed from the untransformed austenite during the

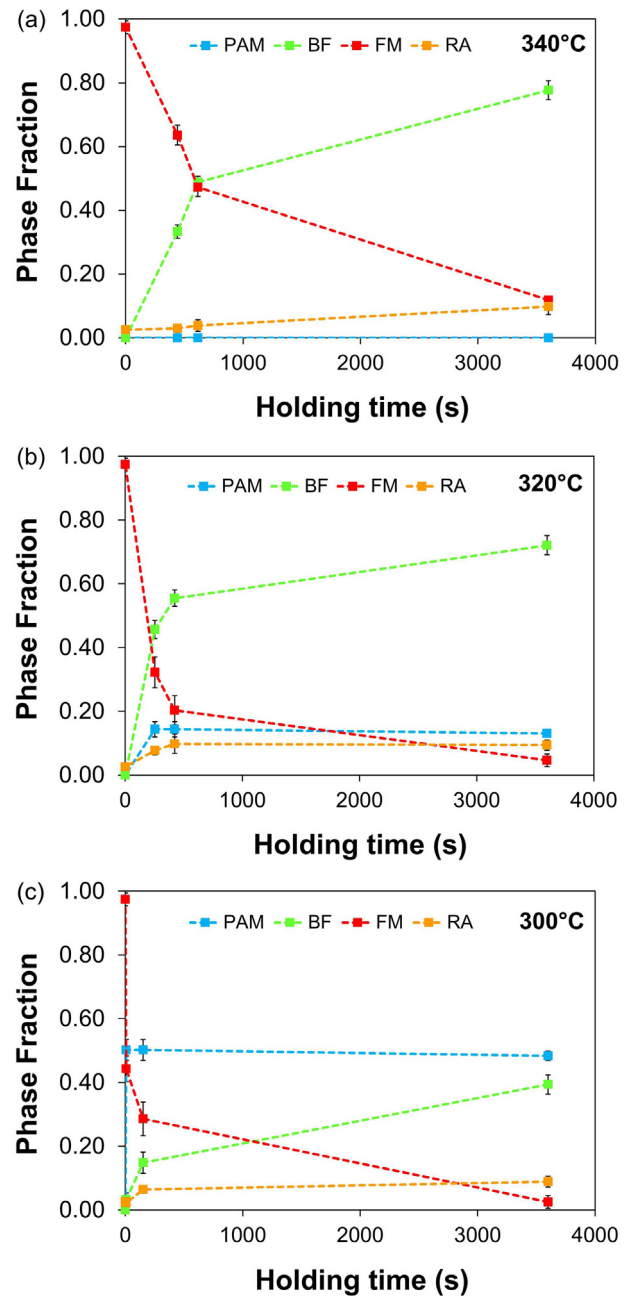
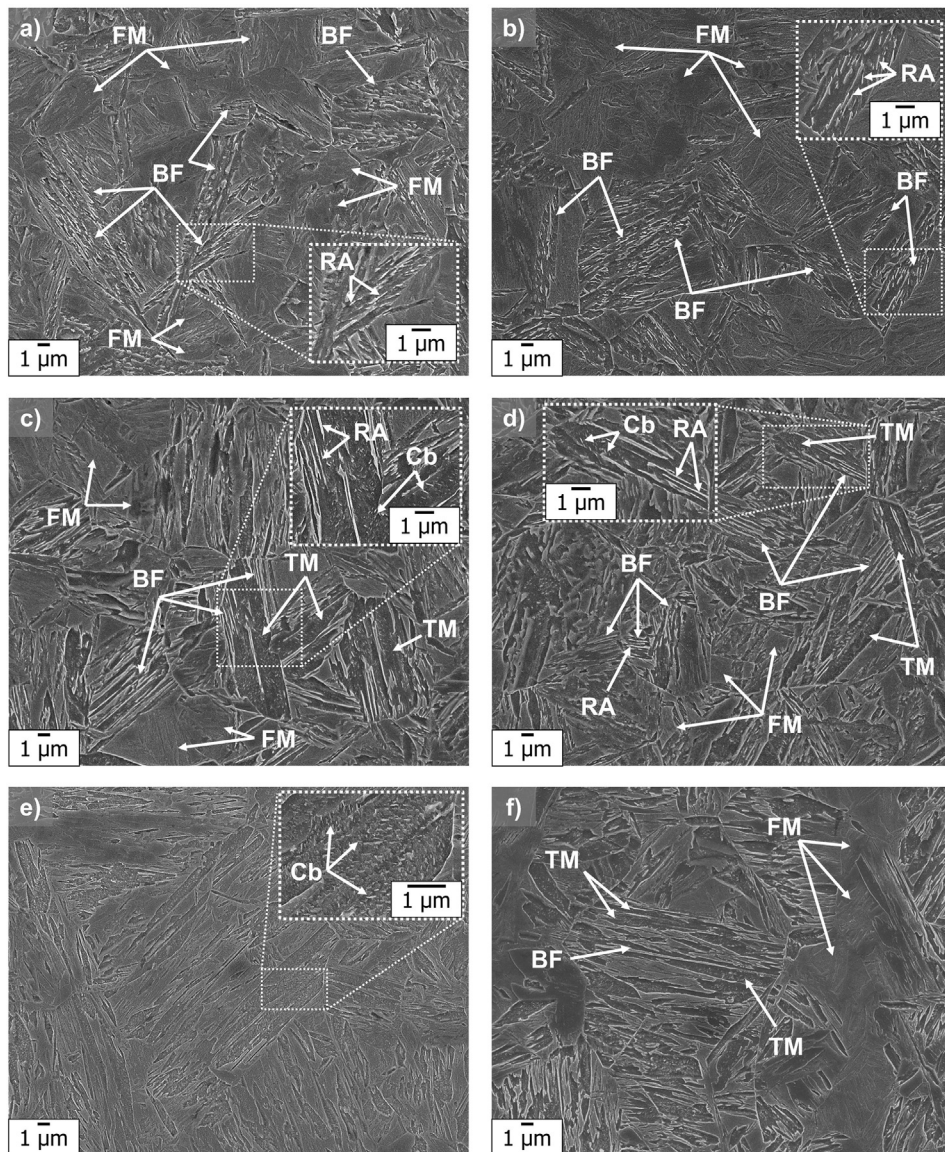


Fig. 4. Evolution of the multiphase mixture after the application of isothermal treatments at (a) 340 °C, (b) 320 °C, and (c) 300 °C for holding times 't1', 't2', and 't3'. The phase mixture of the direct quenched specimen is considered in all figures as the reference value at holding time '0 s'. The following terms refer to: 'PAM: prior athermal martensite', 'BF: bainitic ferrite', 'FM: fresh martensite', and 'RA: retained austenite'.

final cooling to room temperature. The final fraction of retained austenite also increases with holding time at all temperatures, reaching maximum values of 0.10 in specimens heat treated for 1 h of holding time.

### 3.2. Microstructural evolution

The microstructural characterization of the direct-quenched specimen and specimens isothermally treated at the selected temperatures for the holding time 't3' is presented in a previous work of the present authors [18]. Fig. 5 shows the microstructures obtained in specimens heat treated by isothermal holdings 't1' and 't2' at temperatures above and below  $M_s$ . At 340 °C (above  $M_s$ ), the microstructure evolves from a martensitic matrix, formed by large fresh martensite (FM) areas



**Fig. 5.** Evolution of microstructures obtained from different isothermal holding times at temperatures of a-b) 340 °C (t1-t2), c-d) 320 °C (t1-t2), and e-f) 300 °C (t1-t2). The following terms refer to: 'TM: tempered martensite', 'BF: bainitic ferrite', 'FM: fresh martensite', 'RA: retained austenite', and 'Cb: carbides'. In this work, the term TM refers to PAM which is tempered during isothermal holding.

surrounded by small acicular units of bainitic ferrite (BF) after a holding time of 441 s ('t1') (see Fig. 5a), to a bainitic-martensitic matrix of similar phase fractions, where bainitic ferrite and fresh martensite appear in the form of acicular units and laths, respectively, after a holding time of 615 s ('t2') (see Fig. 5b). Retained austenite is present in the form of thin films between the units of bainitic ferrite, as observed in the dashed-rectangular magnified area of Fig. 5a-b.

At 320 °C (below  $M_s$ ), tempered martensite (TM) is present in the microstructure since a 14% volume fraction of prior athermal martensite is formed before applying the isothermal holdings. After the holding time of 253 s ('t1') (Fig. 5c), there is a bainitic-martensitic matrix of similar phase fractions formed by acicular units of bainitic ferrite with thin films of retained austenite between them, besides tempered martensite and fresh martensite laths. When the applied holding time is 422 s ('t2') (Fig. 5d), the martensitic-bainitic matrix evolves towards a matrix that is mainly formed by bainitic ferrite units. In both microstructures, tempered martensite is characterized by large elongated laths with carbides (Cb). Since the austenite regions untransformed during the isothermal holding are reduced from the isothermal treatment 't1' to 't2', laths of

fresh martensite become smaller, and large fresh martensite areas are progressively converted into isolated martensite-austenite (MA) islands.

At 300 °C (below  $M_s$ ), prior athermal martensite represents a 50% volume fraction of the final microstructure. After the heat treatment 't1' (see Fig. 5e), in which the holding time is only 7 s, the microstructure is similar to the one obtained in a direct-quenched specimen (see ref. [18]). Carbides (Cb) are present within the martensite laths, as observed in the dashed-rectangular magnified area of Fig. 5e, which indicates possible auto-tempering of martensite. Despite obtaining similar fractions of prior athermal martensite (PAM) and fresh martensite, approximately 50% and 44%, respectively, the microstructural characteristics defining tempered martensite at higher temperatures cannot be distinguished in this microstructure. Moreover, it is not possible to ascertain the presence of bainitic ferrite due to its small volume fraction (<5%). For the heat treatment 't2', in which the holding time is increased to 151 s, tempered martensite can be distinguished from fresh martensite (see Fig. 5f). Tempered martensite is present as elongated laths and laths with a sharp tip at one of its edges. Both types of martensitic laths contain carbides. Small bainitic ferrite units are identified in the

surroundings of tempered martensite laths. Large areas of fresh martensite are also observed in this microstructure.

### 3.3. Mechanical behaviour

Fig. 6a, c, e show the engineering stress-strain curves obtained from uniaxial tensile tests performed to the specimens heat treated for the selected isothermal temperatures and holding times. As observed in these engineering curves, all specimens exhibit a continuous yielding behaviour in spite of differences in the phase mixture obtained after the application of distinct isothermal treatments. This means that there is a smooth transition from elastic to plastic behaviour in all specimens, but the 0.2% yield stress is unambiguous. Extracted from these engineering curves, the evolution of the yield stress (YS) as well as the ultimate tensile strength (UTS) with holding time at the selected temperatures is presented in Fig. 6b, d, f. The yield stress as well as the ultimate tensile strength decrease with holding time, independently of the applied isothermal temperature.

Fig. 6 also shows mean values of uniform elongation (UEL) and strain hardening ('YS/UTS' ratio) of all heat-treated specimens at the selected temperatures. Uniform elongation increases with holding time for all isothermal holding temperatures. Once the maximum UEL is reached (at UTS), necking takes place within the gauge length until fracture. As observed in Fig. 6, fracture strains of all heat-treated specimens are in the range of 17–23%. Note that the sub-size dimensions of double T-shaped specimens used in this work affect the elongation values obtained in tensile tests since the contribution from the necked region to the overall elongation is greater due to the reduced gauge length of the specimens [22]. Therefore, any comparison of these results with literature data must be performed with care. Concerning the 'YS/UTS' ratio, which represents the potential of a material to be hardened by plastic deformation, all heat treated tensile specimens present similar strain hardening potential. The mentioned ratio varies from 0.65 to 0.75, which are considered typical 'YS/UTS' ratios in multiphase steels [13,23]. The specimens isothermally treated above  $M_s$  present a slight increase of their strain hardening potential with increasing holding time. On the contrary, specimens heat treated below  $M_s$  exhibit a slight

decrease of their strain hardening potential with increasing holding time.

## 4. Discussion

### 4.1. Effect of multiphase microstructure on strength

The evolution of the phase mixture with holding time leads to a decrease of the yield stress (YS) and ultimate tensile strength (UTS) in specimens thermally treated at temperatures above and below  $M_s$  (see Figs. 4 and 6). In specimens heat treated above  $M_s$ , the continuous decrease of YS and UTS with increasing holding times is directly related with a marked increase of the fraction of the softer bainitic ferrite at the cost of the decrease of the fraction of the harder fresh martensite (see Figs. 4a and 6b). In specimens heat treated below  $M_s$ , a similar evolution of YS and UTS is observed up to holding times of 600 s (see Fig. 6d and f). However, for longer holding times, the YS hardly decreases in spite of the formation of a higher fraction of bainitic ferrite and a lower fraction of fresh martensite. This dissimilar yielding behaviour after holding time 't2' should be attributed to the presence of prior athermal martensite (PAM) in the multiphase microstructure of specimens isothermally treated below  $M_s$  compared to that of specimens treated above  $M_s$ .

The observed evolution of the yield stress with holding time in specimens isothermally treated below  $M_s$  is partially in agreement with experimental observations reported by Yan et al. [14] and Zinsaz et al. [17]. Both authors studied the mechanical response exhibited by specimens isothermally treated for several holding times at temperatures below  $M_s$  in similarly compositional low-carbon steels as the one investigated in this study. In both investigations, there is a decrease of the YS exhibited by specimens treated below  $M_s$  up to short holding times (approximately 100 s). As the holding time is increased, the yielding response of these specimens radically changes and the YS increases continuously. Both authors suggest that the tempering of a high fraction of PAM dictates the yielding response of these specimens.

For a better comprehension of the yielding behaviour of PAM formed in isothermal treatments below  $M_s$ , the derivative of the true stress-strain curves, which represents the instantaneous work hardening rate ( $\Theta$ ), as a function of the true stress, known as the extended (since

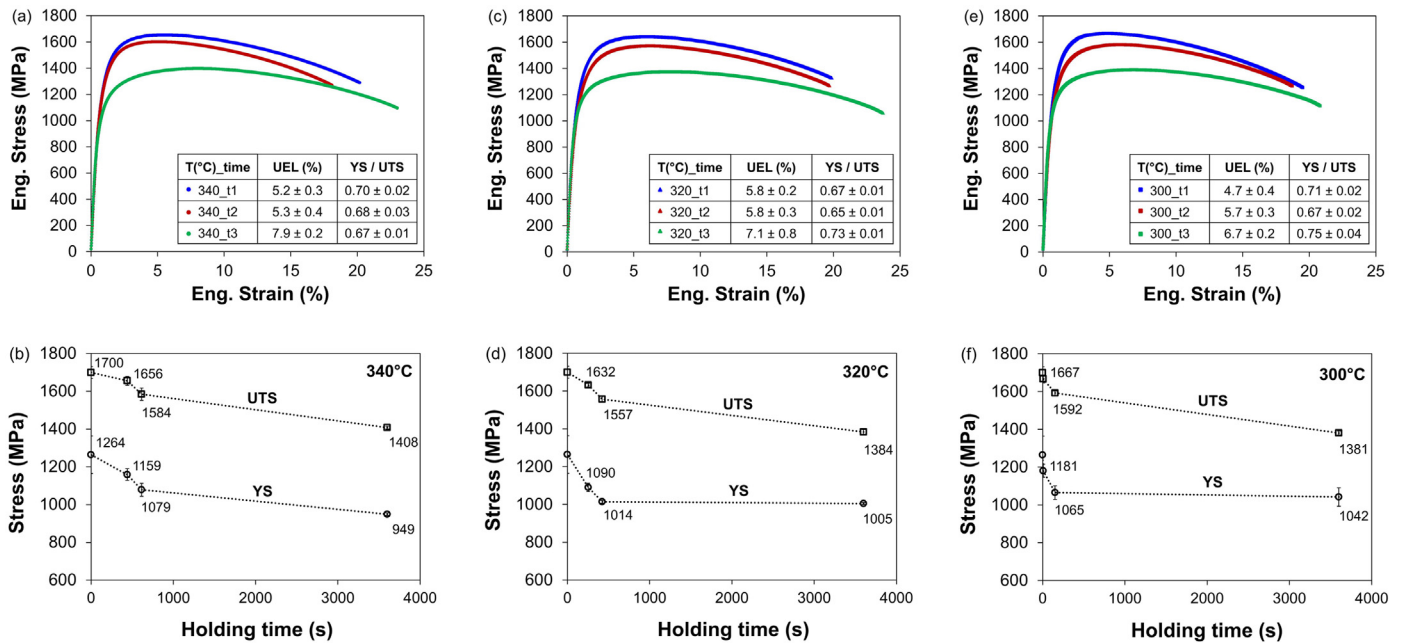


Fig. 6. Engineering stress-strain curves and evolution of 0.2% offset yield stress (YS) and ultimate tensile strength (UTS) of specimens isothermally treated for holding times 't1', 't2', and 't3' at (a–b) 340 °C, (c–d) 320 °C, and (e–f) 300 °C, respectively. Average values of uniform elongation (UEL) and strain hardening ('YS/UTS' ratio) of these specimens are also indicated for each thermal condition. The phase mixture of the direct quenched specimen is considered as the reference value at holding time '0 s'.

also the pre-yield range is included [24]) Kocks-Mecking (K-M) curves [25], is used in this analysis. Extended K-M curves have been demonstrated to be a reliable physically based method, alternative to the 0.2% offset criterion, to determine the yield stress of single-phase ferritic steels [24]. For such materials, two stages are commonly distinguished before uniform elongation is exceeded: 1) a gradual, although initially slow, decay of  $\Theta$  corresponding with the anelastic reversible behaviour due to bowing of dislocations, and 2) a marked transition to the plastic regime when dislocations begin to massively multiply.

Fig. 7a-b show the instantaneous work hardening rate ( $\Theta$ ) of the specimens heat treated at temperatures of 340 °C and 300 °C, respectively. The extended K-M curves of a direct-quench specimen, and quenched and tempered (Q&T) specimens heat treated at both temperatures are also included for comparison. These latter treatments consisted of a one-hour holding stage (tempering) at either 340 °C or 300 °C after a rapid cooling from full austenitization. Both Q&T specimens exhibited a final microstructure which consisted of 97–98% of tempered martensite with 2–3% of retained austenite.

In quenched specimens, the extended Kocks-Mecking curves exhibit an almost linear behaviour beyond stresses of 800 MPa, so no clear transition from elastic to plastic regime is visible. As the microstructure is only formed by quenched martensite, this yielding behaviour is related to the high density of dislocations within this phase together with a probably heterogeneous distribution of dislocation segment lengths. On the other hand, Q&T specimens exhibit extended Kocks-Mecking curves in which the pre-yield and plastic stages are well defined, showing a marked transition between both. The true stress at which an abrupt change of the instantaneous work hardening rate occurs (marked by a red circle in Fig. 7a-b) coincides with the yield stress of

these specimens [24]. This yielding behaviour is related to all processes inherent to tempering, such as segregation/precipitation of carbon and reduction of dislocations density, which structurally modifies the initial matrix of as-quenched martensite [26].

Regarding isothermally treated specimens, the initial very slow decrease of  $\Theta$  is barely observed, but a continuous decay of  $\Theta$  is taking place. Values of  $\Theta$  at very low stresses which exceed typical elastic modulus of around 210 GPa (the shaded range in Fig. 7a-b) arise from inaccuracies of the measurements. The lack of a clear transition from stage 1 to stage 2 denotes continuous yielding, which is typical of martensitic steels, but, for the current alloys, it is also a consequence of a multiphase microstructure. Differences in the shape of the extended K-M curves of the different heat-treated specimens are related with the different mixture of product phases formed after the application of the thermal treatments.

In Fig. 7a, the specimen isothermally treated above  $M_s$  for 't1' exhibits an evolution of  $\Theta$  similar to the direct-quenched specimen since fresh martensite is the dominant phase in the mixture (see Fig. 4a). The same yielding behaviour is observed in the specimen isothermally treated for 't2'. In this case, although the phase mixture evolves to a martensitic-bainitic matrix of similar volume fractions, the harder character of the fresh martensite prevails and, consequently, determines the overall yielding behaviour. However, in the specimen isothermally treated for 1 h ('t3'), where the volume fraction of bainitic ferrite is 78%, the instantaneous work hardening rate decreases faster during stage 1 of the extended K-M curve. This is an indication that bainitic ferrite yields at lower stress than fresh martensite, and its yielding behaviour prevails over the one of the fresh martensite.

In Fig. 7b, the specimen isothermally treated below  $M_s$  for 't1' also exhibits an evolution of  $\Theta$  similar to the direct-quench specimen. This means that, after the formation of 48% volume fraction of PAM, a holding time of 7 s ('t1') is not sufficient to temper it, which indicates that PAM mechanically behaves as fresh martensite for these thermal conditions. In the specimen isothermally treated for 't2', a higher volume fraction of bainitic ferrite is formed (15%), but the overall yielding behaviour is still dominated by martensitic phases, either the harder fresh martensite (29%) or the softer PAM (50%), which is tempered to a certain degree. When the holding time is increased up to 1 h ('t3'), the isothermally treated specimen exhibits a decay of  $\Theta$  before yielding most comparable to the one exhibited by the Q&T specimen (see Fig. 7b). The similarity of both curves is consequence of the presence of a higher fraction (48%) of PAM tempered to a moderate degree, which becomes the dominant phase within the martensitic-bainitic mixture. However, two differences can be observed by comparing both extended K-M curves. The first is that the transition from the elastic to the plastic regime is not yet clearly marked as it is in the extended K-M curve of the Q&T specimen. The second difference is that the gradual decay of  $\Theta$  occurs at lower stress. This is due to the presence of bainitic ferrite in the phase mixture, which indicates that bainitic ferrite yields at lower stress than tempered martensite.

According to this analysis, and taking into consideration the reported results in refs. [14,17], the tempering of PAM strongly affects its yielding behaviour, giving rise to a general decrease of the YS of specimens isothermally treated below  $M_s$  for short holding times (<200 s). Tempering leads to the loss of carbon atoms in solid solution contained in the initial carbon-supersaturated PAM via diffusion into the surrounding untransformed austenite during holding and segregation to the dislocation strain fields in the PAM [27,28]. These processes entail the softening of this product phase and, as a consequence, the decrease of the overall YS and UTS. The precipitation of carbon atoms in the form of carbides, a phenomenon that is also associated to tempering, will be minor during the isothermal holding since, in the present work, the formation of carbides within the PAM already takes place during the initial cooling before the isothermal holding. Fig. 5e shows the early precipitation of carbides in the specimen isothermally treated at 300 °C (below  $M_s$ ) for 7 s ('t1'), confirming the auto-tempering of PAM. On the other

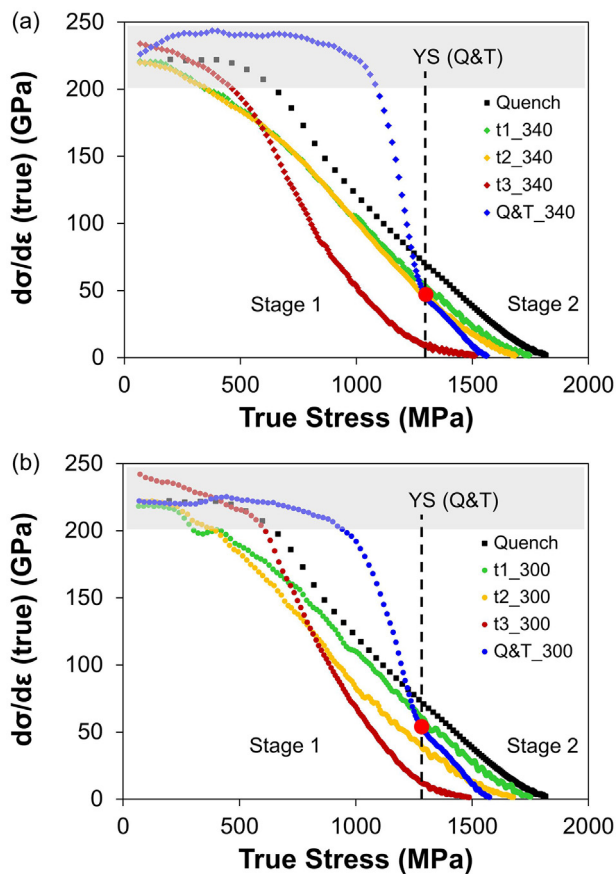


Fig. 7. Instantaneous work hardening rate ( $\Theta$ ) as function of true stress of specimens thermally treated by a rapid cooling ('Quench'), isothermal holdings for several times ('t1', 't2', and 't3'), and quenching and tempering ('Q&T') at temperatures of (a) 340 °C (above  $M_s$ ) and (b) 300 °C (below  $M_s$ ).



hand, the recovery process, which implies the reduction of the dislocation density, can contribute to the softening of the PAM with a moderate degree of tempering, but this effect may be minor in comparison with the ones previously described since the isothermal temperatures applied are lower than 400 °C, the limit temperature above which the recovery of dislocations certainly becomes an important effect of the tempering [29].

As the applied holding time increases (>200 s), it is presumable that processes leading to the softening of PAM are mostly finished, thus the yielding behaviour of PAM does not significantly vary with holding time, becoming similar to the tempered martensite of typical Q&T treatments. The insignificant variation of the yielding behaviour of PAM partially leads to the nearly constant YS exhibited by specimens treated below  $M_s$  after a certain holding time ('t2'). This fact is in agreement with the results reported by Cupertino et al. [30] and Liu et al. [31], concerning the yielding response of Q&T specimens of similarly compositional steels as the one investigated in this study. In both studies, results show that the yield stress of these Q&T specimens remains nearly constant after the application of a certain holding time at tempering temperatures below 350 °C.

In addition to the minor effect of the tempering on the yielding response of the PAM at low temperatures and long holding times, the nearly constant YS in specimens heat treated below  $M_s$  after a certain holding time ('t2') is supported by the smaller variation of bainitic ferrite and fresh martensite fractions between holding times 't2' and 't3' in these specimens, compared to those treated above  $M_s$ . However, this fact does not explain by itself the nearly constant YS since, in principle, the formation of bainitic ferrite at the cost of fresh martensite should lead to the reduction, to some extent, of the YS and UTS of specimens isothermally treated below  $M_s$ . For these specimens, the strengthening effect due to the refinement of bainitic structures may partially counteract the expected decrease of YS [18].

The higher refinement of bainitic structures with the decreasing temperature has been experimentally reported in conventional low-carbon bainitic steels obtained above  $M_s$  [32,33]. This refinement stems from the higher nucleation rate of bainitic ferrite due to the larger driving force for its formation at lower temperatures and from the larger resistance of the untransformed austenite to the motion of bainite-austenite interfaces [32]. However, the strengthening caused by the refinement of bainitic structures is further enhanced in specimens isothermally treated below  $M_s$  due to the formation of PAM before the bainite reaction. This fact leads to the initial formation of finer bainitic structures, compared to specimens isothermally treated above  $M_s$ , due to the fragmentation of the initial austenite grains [15] and the higher strengthening of the untransformed austenite as consequence of the dislocations introduced by the martensitic transformation. These dislocations will be inherited by the further formed bainitic ferrite [34], resulting into a higher overall strengthening in terms of YS of the specimens isothermally treated below  $M_s$  and, consequently, maintaining a nearly constant YS with holding time.

The extended K-M curves have been demonstrated to be a powerful method to analyse the mechanical response of these advanced multiphase steels since relevant differences in terms of yielding were observed between heat treated specimens containing PAM with different degrees of tempering. This new approach can thus give reliable information concerning the mechanical response of the bainitic phase formed below  $M_s$ . Fig. 8 shows the extended K-M curves of the specimens isothermally treated for the holding time 't3' at the three selected temperatures. As observed, the specimens treated at 340 °C (above  $M_s$ ) and 320 °C, (below  $M_s$ ) with a similar high fraction of bainitic ferrite in their microstructure exhibit nearly the same yielding behaviour, i.e., a rapid decay of  $\theta$  at low stress. This mechanical response is similarly reproduced in the specimen treated at 300 °C, below  $M_s$ , where a considerable fraction of bainitic ferrite is present.

This unique observation via the K-M curves confirms, from the point of view of the mechanical behaviour, that the isothermal product

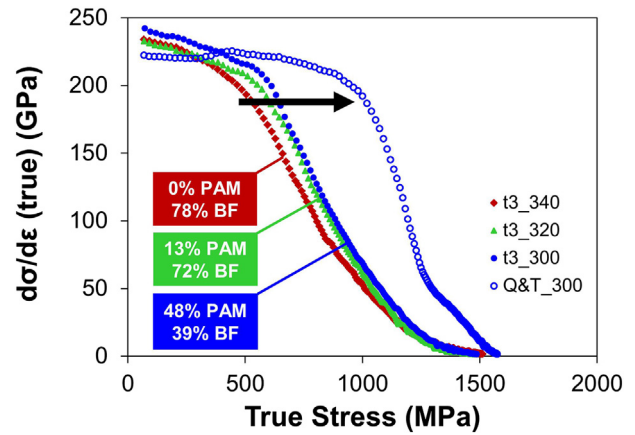


Fig. 8. Extended K-M curves of specimens isothermally treated for the holding time 't3' at the selected temperatures above and below  $M_s$ . The corresponding K-M curve of the specimen quenched and tempered at 300 °C for 1 h has been included for comparison.

formed below  $M_s$  has a bainitic character since the yielding behaviour of microstructures isothermally obtained below  $M_s$  resembles well that of bainitic microstructures obtained above  $M_s$ . However, the formation of a certain fraction of PAM, tempered to a certain degree during the isothermal holding, modifies the yielding behaviour of the bainitic microstructures by delaying the rapid decay of  $\theta$  to higher stress, as indicated by a black arrow in Fig. 8. This yielding behaviour may progressively evolve towards the one exhibited by Q&T specimens by increasing the volume fraction of PAM formed before the isothermal bainite reaction starts. Further investigations are needed to determine the volume fraction of PAM at which the yielding behaviour of the multiphase microstructure becomes similar to that of a fully tempered martensite.

#### 4.2. Effect of multiphase microstructure on strain hardening

Uniform elongation increases with holding time in all heat treated specimens above and below  $M_s$ , as shown in Fig. 6a,c,e. This is due to the balanced evolution of product phases with holding time, in which the fraction of softer bainitic ferrite increases at the cost of the harder martensite formed during the final cooling after the isothermal holding. On the other hand, below  $M_s$ , the strain hardening potential slightly decreases with holding time, as opposed to what it is observed in isothermal treatments above  $M_s$ . This decrease may be consequence of three phenomena. The first two phenomena are presumably related to the pinning effect of dislocations derived from the precipitation of carbides within PAM and the grain refinement of bainitic structures occurring in specimens isothermally treated below  $M_s$ . The presence of carbides and finer structures can partially hinder the movement of dislocations until a higher level of tensile stress is reached [26]. The constrained movement of dislocations certainly contributes to a higher strengthening in terms of YS. However, further investigations are required for a better understanding of the hindering effect caused by both phenomena on the dislocation motion occurring within each phase contained in these multiphase specimens.

The third phenomenon derives from the softening of the phase mixture with holding time, leading to the decrease of UTS. This decrease is consequence of the formation of higher fractions of bainitic ferrite and lower fractions of fresh martensite, but also of the softening of PAM during tempering due to the partial loss of carbon contained in solid solution and the likely reduction of its dislocation density. For multiphase steels obtained by isothermal treatments below  $M_s$ , it can be assumed that the maximum carbon concentration in solid solution within PAM corresponds to that estimated from quenching and tempering (Q&T) treatments performed at the same isothermal temperature and holding time. Taking into consideration this assumption and following the

experimental procedure described in [18], the carbon concentration in solid solution within PAM can be drastically reduced during one-hour tempering (as reported in [18]), mainly due to carbon precipitation as carbides and carbon partitioning into other phases. The combined effect of the three described phenomena gives as result the increase of the 'YS/UTS' ratio, i.e., the decrease of the strain hardening potential in specimens isothermally treated below  $M_s$ .

The decrease of the strain hardening capacity can be partially counteracted by the mechanically-induced transformation of the retained austenite into martensite during the application of stress. This austenite-to-martensite transformation generally occurs within the uniform plastic deformation regime delaying the beginning of the necking, which implies an increase of the UTS. However, this counteracting effect on the UTS is challenging to be quantitatively analysed due to the complexity of the multiphase mixture created from these heat treatments. Investigations on the mechanical stability of the retained austenite in specimens isothermally treated for a holding time of 't3' at the same temperatures above and below  $M_s$  show a similar contribution of the retained austenite to the strain hardening capacity in all specimens [18]. This is attributed to the similar mechanical stability of the retained austenite as consequence of a similar carbon concentration (see Table 3), which leads to the mechanical transformation of approximately two thirds of the total fraction of retained austenite during the uniaxial tensile tests [18].

In the present work, the formation of similar retained austenite fractions with comparable carbon enrichment, especially for 't2' holding times (see Table 3), may lead to a similar effect of the mechanically-induced transformation of the retained austenite on the strain hardening in all heat treated specimens. However, the decreasing evolution of the strain hardening capacity from 't2' to 't3' holding times (below  $M_s$ ) suggests that this transformation-induced effect cannot counteract by itself the opposing effects previously described that negatively affect the capacity of specimens isothermally treated below  $M_s$  to be hardened by deformation. Further research is needed to quantitatively determine the contribution of the distinct morphologies (film-like or blocky) of retained austenite to the strain hardening of these multiphase steels.

4.3. Technological implications

Fig. 9a shows the comparison of microstructure and properties of the specimens heat treated at two of the selected temperatures, 340 °C (above  $M_s$ ) and 320 °C (below  $M_s$ ), during similar holding times (441 s and 422 s, respectively). A higher fraction of bainitic ferrite is isothermally formed at 320 °C compared to the volume fraction formed at 340 °C during a similar holding time. This is mainly a consequence of the increasing number of preferential sites for bainite nucleation introduced as martensite-austenite interfaces due to the formation of PAM before the bainite reaction [3,6]. The presence of these newly-created preferential sites triggers an accelerating effect in the kinetics of the bainitic ferrite formation at 320 °C in comparison with the kinetics of the bainite

Table 3

Volume fraction of retained austenite ( $f^{RA}$ ) and its carbon concentration ( $X_C^{RA}$ ) in wt% in specimens isothermally treated at 340 °C, 320 °C, and 300 °C for different holding times ('t1', 't2', 't3') before the application of tensile tests. The carbon concentration of retained austenite at room temperature was calculated according to the equation reported in ref. [35].

| T (°C) | time        | $f^{RA}$    | $X_C^{RA}$ (%) |
|--------|-------------|-------------|----------------|
| 340    | t1 (441 s)  | 0.03 ± 0.01 | 0.79 ± 0.09    |
|        | t2 (615 s)  | 0.04 ± 0.02 | 0.85 ± 0.09    |
|        | t3 (3600 s) | 0.10 ± 0.03 | 0.91 ± 0.06    |
| 320    | t1 (253 s)  | 0.08 ± 0.01 | 0.79 ± 0.09    |
|        | t2 (422 s)  | 0.10 ± 0.03 | 0.85 ± 0.09    |
|        | t3 (3600 s) | 0.09 ± 0.02 | 0.91 ± 0.03    |
| 300    | t1 (7 s)    | 0.02 ± 0.01 | 0.79 ± 0.09    |
|        | t2 (151 s)  | 0.06 ± 0.01 | 0.79 ± 0.09    |
|        | t3 (3600 s) | 0.09 ± 0.02 | 0.85 ± 0.06    |

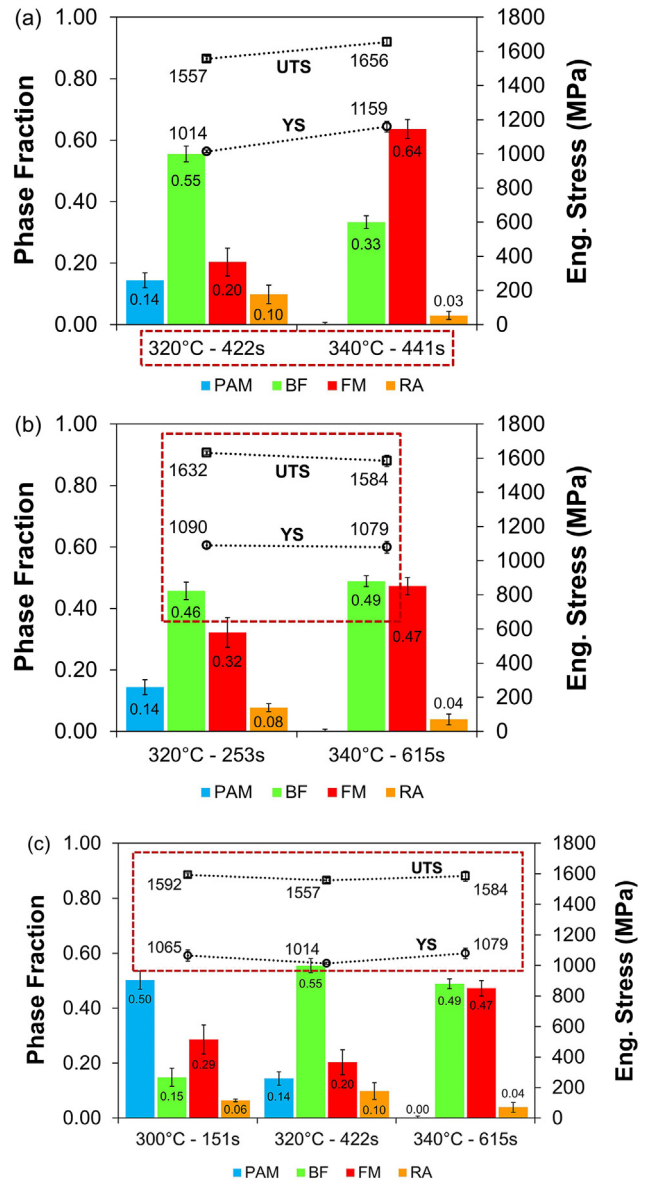


Fig. 9. Comparison of the microstructure-properties relationships between specimens isothermally treated at distinct temperatures above and below  $M_s$  (a) for a similar holding time, (b) containing a similar bainite fraction, and (c) exhibiting similar yield stress and ultimate tensile strength.

reaction occurred at 340 °C, where there is no presence of PAM. A higher formation of bainitic ferrite at 320 °C subsequently leads to the formation of a lower fraction of fresh martensite during the final cooling after the isothermal holding. The resulting multiphase microstructure, where bainitic ferrite becomes the dominant phase, gives rise to a decrease of 100–150 MPa of the YS and UTS, as well as an increase of the uniform elongation and the strain hardening capacity, with respect to the multiphase microstructure formed above  $M_s$ .

In Fig. 9b, the comparison is made between two specimens with similar fractions of bainitic ferrite (approx. 46–49%), heat treated at the same two temperatures above and below  $M_s$ , 340 °C and 320 °C, respectively. Due to the accelerated kinetics of bainite reaction derived from the formation of PAM, there is a strong reduction of the isothermal holding time applied at 320 °C to obtain a similar bainitic ferrite fraction to that obtained at 340 °C. Comparable YS and UTS are exhibited by both types of heat-treated specimens, although the difference in UTS is not negligible. According to these comparisons, the formation of martensite prior to the subsequent bainite reaction below  $M_s$  leads to a drastic

**Table 4**  
Chemical composition, specimen dimensions, and original tensile data of several steels heat treated by isothermal treatments above and below  $M_s$  ( $L_{0k}$ ,  $w_{0k}$ , and  $z_{0k}$  are the gauge length, width, and thickness, respectively (in mm) of the tensile specimens; UTS: ultimate tensile strength (MPa); TEL: total elongation (%)).

| Reference    | Alloy composition (wt%)             | $L_{0k}$ | $w_{0k}$ | $z_{0k}$ | Above or below $M_s$ | UTS (MPa) | TEL (%) |
|--------------|-------------------------------------|----------|----------|----------|----------------------|-----------|---------|
| Present work | 0.2C-3.5Mn-1.5Si-0.25Mo-0.04Al      | 10       | 4        | 2        | Above                | 1408      | 21.9    |
|              |                                     |          |          |          |                      | 1584      | 19.7    |
|              |                                     |          |          |          |                      | 1656      | 19.4    |
|              |                                     |          |          |          |                      | 1384      | 23.7    |
|              |                                     |          |          |          | Below                | 1381      | 21.3    |
|              |                                     |          |          |          |                      | 1557      | 18.4    |
|              |                                     |          |          |          |                      | 1592      | 18.4    |
|              |                                     |          |          |          |                      | 1632      | 18.9    |
| [5]          | 0.15C-1.9Mn-1.4Si-1.9Cr-0.4Ni-0.3Mo | 25       | 10       | 3        | Above                | 1667      | 17.8    |
|              |                                     |          |          |          |                      | 1408      | 15.0    |
|              |                                     |          |          |          |                      | 1424      | 21.0    |
|              |                                     |          |          |          | Below                | 1393      | 17.5    |
|              |                                     |          |          |          |                      | 1504      | 19.0    |
|              |                                     |          |          |          |                      | 1400      | 13.2    |
| [11]         | 0.2C-2.5Mn-1.5Si-0.8Cr              | 15       | 9        | 1.4      | Above                | 1360      | 13.2    |
|              |                                     |          |          |          |                      | 1400      | 19.6    |
|              |                                     |          |          |          | At $M_s$             | 1300      | 17.9    |
|              |                                     |          |          |          |                      | 1490      | 15.4    |
|              |                                     |          |          |          | Below                | 1290      | 15.1    |
|              |                                     |          |          |          |                      | 1570      | 15.2    |
| [12]         | 0.2C-1.7Mn-1.7Si-0.2 V              | 20       | 12.5     | 4        | Below                | 1336      | 14.3    |
|              |                                     |          |          |          |                      | 1323      | 14.6    |
|              |                                     |          |          |          |                      | 1229      | 14.3    |
|              |                                     |          |          |          |                      | 1215      | 11.5    |
|              |                                     |          |          |          |                      | 1142      | 10.2    |
| [15]         | 0.4C-0.82Mn-0.35Si-0.9Cr-0.1Mo      | 100      | 13       | 6        | Above                | 1586      | 8.7     |
|              |                                     |          |          |          |                      | 1333      | 5.6     |
|              |                                     |          |          |          |                      | 1452      | 13.2    |
|              |                                     |          |          |          | Below                | 1684      | 14.5    |
|              |                                     |          |          |          |                      |           |         |

reduction of the holding time needed to form similar fractions of bainitic ferrite as those formed above  $M_s$ , maintaining comparable mechanical properties between the specimens isothermally treated at both temperatures.

Finally, Fig. 9c shows the comparison of microstructure and properties of specimens exhibiting similar values of YS and UTS. The specimens isothermally treated at the lowest temperature (300 °C) applying the shortest holding time (151 s) show intermediate values of YS and UTS compared to those exhibited by the other two specimens isothermally treated at higher temperatures and longer holding times. This implies a further step in the development of advanced multiphase steels with a bainitic-martensitic matrix. In this case, similar mechanical properties in terms of strength (YS and UTS), as well as of uniform elongation and strain hardening (see Fig. 6), can be achieved with much shorter processing times by obtaining microstructures where bainitic ferrite is no longer the dominant phase, giving a greater relevance to the PAM with a certain degree of tempering.

The present study shows that the martensitic-bainitic steels developed by isothermal treatments above  $M_s$  can be replaced by those developed below  $M_s$  without compromising the mechanical performance under tensile deformation. To benchmark this new family of advanced high strength steels, the mechanical properties obtained in the present work through the application of isothermal treatments above and below the  $M_s$  temperature in a low-carbon high-silicon steel are compared with those obtained in similar thermal cycles and chemical compositions by other researchers [5,11–13,15]. Table 4 shows the original data extracted from the referenced works. Due to the use of different sub-size specimens, the values of total elongation were corrected by a simplified form of the Oliver formula [36], which is currently adopted by the existing standardised methodology [37]. This formula is expressed as

$$A_c = A_k \cdot \left( \frac{L_{0k}}{\sqrt{S_{0k}}} \right)^n \cdot \left( \frac{\sqrt{S_{0c}}}{L_{0c}} \right)^n \quad (1)$$

where  $A_c$  and  $A_k$  are the corrected and observed elongations,  $L_{0k}$  and  $S_{0k}$

are the gauge length and cross-section of the sub-size specimens, and  $L_{0c}$  and  $S_{0c}$  are the gauge length and cross-section obtained from the ASTM standards [38]. In this case, according to ASTM25, the standard specimen dimensions are: gauge length ( $L_{0c}$ ) of 25 mm, width ( $w_{0c}$ ) of 6.04 mm, and thickness ( $z_{0c}$ ) of 3 mm, which implies  $S_{0c} = 18 \text{ mm}^2$ . These dimensions were selected taking into consideration previous studies on the influence of the specimen dimensions on the tensile elongation of advanced high strength steels [39,40]. The exponent  $n$  is a geometrically dependent parameter that it is usually taken as 0.4 [36].

The corrected values of total elongation (TEL) of all specimens in relation to their ultimate tensile strength (UTS) are included in the steel properties diagram of Fig. 10. As observed, the mechanical properties obtained in the present work are comparable to the ones obtained in similar studies performed with low-C steels. Therefore, new advanced

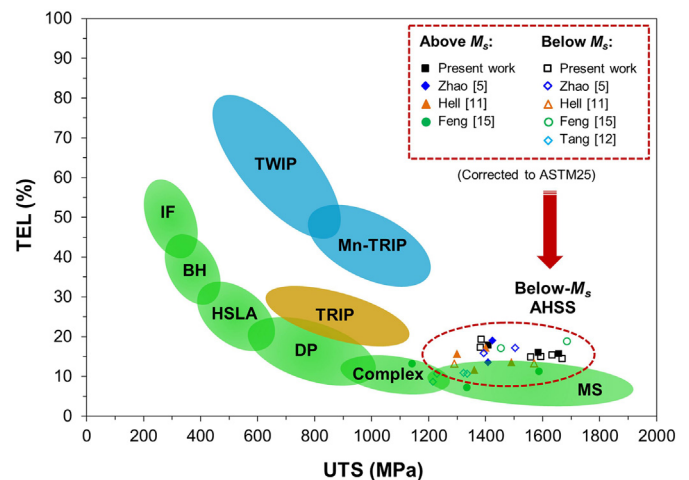


**Fig. 10.** Diagram of steel properties in which the newly-designed advanced high strength steels (AHSS) through isothermal holdings below  $M_s$  are included [41]. Conventional bainitic steels isothermally obtained above  $M_s$  are displayed for comparison. Values of total elongation (TEL) were corrected according to the standardised methodology.

high strength steels based on the presented approach can lead to a competitive advantage for steel industry, since faster processing and, thus, more sustainable routes can be implemented through isothermal holdings below  $M_s$  to manufacture steels with mechanical properties comparable to those obtained by conventional treatments above  $M_s$ .

## 5. Conclusions

The relationships between microstructure and properties of different multiphase microstructures obtained through the application of isothermal holdings at temperatures above and below  $M_s$  in a low-C high-Si steel are analysed at different holding times up to 1 h. The microstructure-properties relationships are globally benchmarked within the family of advanced high strength steels (AHSS). The main conclusions obtained are the following:

1. The degree of tempering of prior athermal martensite with holding time has a primary effect on the overall mechanical response of specimens heat treated below  $M_s$ . Prior athermal martensite yields as quenched martensite after short holding times (<200 s), whereas its yielding behaviour becomes comparable to that of tempered martensite as the holding time is increased.
2. Analysing the mechanical response by extended Kocks-Mecking plots confirms that the isothermal product formed below  $M_s$  has a bainitic character. The increased formation of bainitic ferrite within the phase mixture leads to a faster decrease of the instantaneous work hardening at low stresses, indicating that bainitic ferrite yields at lower stress than fresh martensite and tempered martensite.
3. The yield stress of multiphase microstructures formed below  $M_s$  remains practically unchanged with holding time after the first minutes compared to the progressive decrease of the yield stress with holding time observed in conventional bainitic steels. Also, an opposite evolution of the strain hardening capacity is observed between both types of multiphase steels. The mechanical response of multiphase microstructures formed below  $M_s$  is a direct consequence of the microstructural refinement, carbide precipitation, and matrix softening, which are phenomena derived from the formation and tempering of prior athermal martensite.
4. Combinations of product phases can be tailored varying processing temperatures and times in treatments below  $M_s$  to manufacture steels grades with similar properties to those obtained by conventional heat treatments performed above  $M_s$ , but with a considerable reduction in energy consumption. This energetic advantage stems from shorter processing times as a consequence of the accelerating effect of prior athermal martensite on the subsequent bainite reaction.

## CRedit authorship contribution statement

**Alfonso Navarro-López:** Conceptualization, Investigation, Formal analysis, Writing - original draft, Visualization. **Javier Hidalgo:** Formal analysis, Supervision, Writing - review & editing. **Jilt Sietsma:** Supervision, Writing - review & editing, Funding acquisition. **Maria J. Santofimia:** Conceptualization, Resources, Supervision, Writing - review & editing, Project administration, Funding acquisition.

## Declaration of competing interest

The authors declare that they have no known competing financial interests or personal relationships that could have appeared to influence the work reported in this paper.

## Acknowledgements

The authors wish to thank Dr. Zaloa Arechabaleta for the fruitful discussions on extended Kocks-Mecking curves, and Richard Huizenga for

the X-ray diffraction measurements. This research work was financially supported by the Netherlands Organisation for Scientific Research (NWO) as well as by the Dutch Foundation for Applied Sciences (STW) through the VIDI-Grant 12376.

## Data availability

The raw and processed data required to reproduce the findings of this research study are available to download from <https://doi.org/10.4121/uuid:1d4b3727-825e-452d-9a89-c8712ac1198>.

## References

- [1] R.T. Howard, M. Cohen, Austenite transformation above and within the martensite range, *Trans. AIME* 176 (1948) 384–397.
- [2] C.E. Ericsson, M.S. Bhat, E.R. Parker, V.F. Zackay, Isothermal studies of bainitic and martensite transformations in some low alloy steels, *Metall. Trans. A* 7 (1976) 1800–1803.
- [3] H. Kawata, K. Hayashi, N. Sugiura, N. Yoshinaga, M. Takahashi, Effect of martensite in initial structure on bainite transformation, *Mater. Sci. Forum* 638–642 (2010) 3307–3312.
- [4] M.J. Santofimia, S.M.C. van Bohemen, D.N. Hanlon, L. Zhao, J. Sietsma, Perspectives in high-strength steels: Interactions between non-equilibrium phases, *Inter. Symp. On AHSS, AIST* 2013, pp. 331–339.
- [5] L. Zhao, L. Qian, J. Meng, Q. Zhou, F. Zhang, Below- $M_s$  austempering to obtain refined bainitic structure and enhanced mechanical properties in low-C high-Si/Al steels, *Scripta Mater* 112 (2016) 96–100.
- [6] A. Navarro-López, J. Sietsma, M.J. Santofimia, Effect of prior athermal martensite on the isothermal transformation kinetics below  $M_s$  in a low-C high-Si steel, *Metall. Mater. Trans. A* 47A (2016) 1028–1039.
- [7] S.M.C. van Bohemen, M.J. Santofimia, J. Sietsma, Experimental evidence for bainite formation below  $M_s$  in Fe-0.66C, *Scripta Mater* 58 (2008) 488–491.
- [8] P. Kolmskog, A. Borgenstam, M. Hillert, P. Hedstrom, S.S. Babu, H. Terasaki, Y.I. Komizo, Direct observation that bainite can grow below  $M_s$ , *Metall. Mater. Trans. A* 43A (2012) 4984–4988.
- [9] E.P. Da Silva, D. De Knijf, W. Xu, C. Föjler, Y. Houbaert, J. Sietsma, R. Petrov, Isothermal transformations in advanced high strength steels below martensite start temperature, *Mater. Sci. Technol.* 31 (2015) 808–816.
- [10] S. Samanta, P. Biswas, S. Giri, S.B. Singh, S. Kundu, Formation of bainite below the  $M_s$  temperature: kinetics and crystallography, *Acta Mater.* 105 (2016) 390–403.
- [11] J.C. Hell, M. Dehmas, S. Allain, J.M. Prado, A. Hazote, J.P. Chateau, Microstructure-properties relationships in carbide-free bainitic steels, *ISIJ Int.* 51 (2011) 1724–1732.
- [12] X. Tan, Y. Xu, X. Yang, D. Wu, Microstructure-properties relationship in a one-step quenched and partitioned steel, *Mater. Sci. Eng. A* 589 (2014) 101–111.
- [13] G. Mandal, S.K. Ghosh, S. Bera, S. Mukherjee, Effect of partial and full austenitisation on microstructure and mechanical properties of quenching and partitioning steel, *Mater. Sci. Eng. A* 676 (2016) 56–64.
- [14] S. Yan, X. Liu, W.J. Liu, T. Liang, B. Zhang, L. Liu, Y. Zhao, Comparative study on microstructure and mechanical properties of a C-Mn-Si steel treated by quenching and partitioning (Q&P) processes after a full and intercritical austenitization, *Mater. Sci. Eng. A* 684 (2017) 261–269.
- [15] J. Feng, T. Frankenbach, M. Wettlaufer, Strengthening 42CrMo4 steel by isothermal transformation below martensite start temperature, *Mater. Sci. Eng. A* 683 (2017) 110–115.
- [16] J. Tian, G. Xu, M. Zhou, H. Hu, Refined bainite microstructure and mechanical properties of a high-strength low-carbon bainitic steel treated by austempering below and above  $M_s$ , *Steel Research Inter* (2018) 1–10.
- [17] A. Zinsaz-Borujerdi, A. Zarei-Hanzaki, H.R. Abedi, M. Karam-Abian, H. Ding, D. Han, N. Kheradmand, Room temperature mechanical properties and microstructure of a low alloyed TRIP-assisted steel subjected to one-step and two-step quenching and partitioning process, *Mater. Sci. Eng. A* 725 (2018) 341–349.
- [18] A. Navarro-Lopez, J. Hidalgo, J. Sietsma, M.J. Santofimia, Influence of the prior athermal martensite on the mechanical response of advanced bainitic steel, *Mater. Sci. Eng. A* 735 (2018) 343–353.
- [19] G. Krauss, Tempering of martensite in carbon steels. Book 'phase transformations in steels, Diffusionless Transformations, High Strength Steels, Modelling and Advanced Analytical Techniques, Volume 2, Woodhead Publishing Limited 2012, pp. 126–150, Chapter 5.
- [20] A. Navarro-López, J. Hidalgo, J. Sietsma, M.J. Santofimia, Characterization of bainitic-martensitic structures formed in isothermal treatments below the  $M_s$  temperature, *Mat. Charact.* 128 (2017) 248–256.
- [21] C.F. Jatzcak, J.A. Larson, S.W. Shin, Retained Austenite and its Measurements by X-Ray Diffraction, Society of Automotive Engineers, 1980 453 (Special Publication).
- [22] G.E. Dieter, *Mechanical Metallurgy*, SI Metric edition McGraw-Hill, 1988.
- [23] E.P. Bagliani, M.J. Santofimia, L. Zhao, J. Sietsma, E. Anelli, Microstructure, tensile and toughness properties after quenching and partitioning treatments of a medium-carbon steel, *Mater. Sci. Eng. A* 559 (2013) 486–495.
- [24] Z. Arechabaleta, P. van Liempt, J. Sietsma, Quantification of dislocation structures from anelastic deformation behaviour, *Acta Mater.* 115 (2016) 314–323.
- [25] U.F. Kocks, H. Mecking, Physics and phenomenology of strain hardening: the FCC case, *Prog. Mater. Sci.* 48 (2003) 171–273.

- [26] G. Krauss, *Steels: Processing, Structure, and Performance*, 2<sup>nd</sup> edition ASM International, Materials Park, OH, USA, 2015 (Chapters 17 & 18).
- [27] M.K. Miller, P.A. Beaven, G.D.W. Smith, A study of the early stages of tempering of iron-carbon martensites by atom probe field ion microscopy, *Metall. Trans. A* 12 (1981) 1197–1204.
- [28] L. Chang, S.J. Barnard, G.D.W. Smith, The segregation of carbon atoms to dislocations in low-carbon martensites: Studies by field ion microscopy and atom probe microanalysis, *Symposium of Fundamentals of Aging and Tempering in Bainitic and Martensitic Steel Products*, ISS, Warrendale, PA 1992, pp. 19–28.
- [29] G.R. Speich, W.C. Leslie, Tempering of steel, *Metall. Trans.* 3 (1972) 1043–1054.
- [30] L.R. Cupertino, E.A. Pachon, A. Arlazarov, Mechanical behaviour of tempered martensite: characterization and modeling, *Mater. Sci. Eng. A* 706 (2017) 38–47.
- [31] D. Liu, B. Bai, H. Fang, W. Zhang, J. Gu, K. Chang, Effect of tempering temperature and carbide free bainite on the mechanical characteristics of a high strength low alloy steel, *Mater. Sci. Eng. A* 371 (2004) 40–44.
- [32] S.B. Singh, H.K.D.H. Bhadeshia, Estimation of bainite plate-thickness in low-alloy steels, *Mater. Sci. Eng. A* 245 (1998) 72–79.
- [33] S.H. He, B.B. He, K.Y. Zhu, M.X. Huang, On the correlation among dislocation density, lath thickness and yield stress of bainite, *Acta Mater.* 135 (2017) 382–389.
- [34] S.H. He, B.B. He, K.Y. Zhu, M.X. Huang, Evolution of dislocation density in bainitic steel: modeling and experiments, *Acta Mater.* 149 (2018) 46–56.
- [35] J.B. Seol, D. Raabe, P.P. Choi, Y.R. Im, C.G. Park, Atomic scale effects of alloying, partitioning, solute drag and austempering on the mechanical properties of high-carbon bainitic-austenitic TRIP steels, *Acta Mater.* 60 (2012) 6183–6199.
- [36] D.A. Oliver, Proposed new criteria of ductility from a new law connecting the percentage elongation with size of test-piece, *Proc. Inst. Mech. Eng.* 2 (1928) 827–864.
- [37] ISO 2566-1, Steel – Conversion of Elongation Values – Part 1: Carbon and Low Alloy Steels, International Organization for Standardization (ISO), Geneva, Switzerland, 1984.
- [38] ASTM E8/E8-09, Standard Test Methods for Tension Testing of Metallic Materials, ASTM International, Philadelphia, PA, 2009.
- [39] G.M. Cola Jr., B. Hanhold, T. Lolla, B. Radhakrishnan, S. Babu, On the tensile elongation of advanced high-strength steels, *AIST Trans* 10 (3) (2013) 1–6.
- [40] D.N. Hanlon, S.M.C. van Bohemen, S. Celotto, Critical assessment 10: tensile elongation of strong automotive steels as function of testpiece geometry, *Mat. Sci. & Techn.* 31 (2015) 385–388.
- [41] [www.dierk-raabe.com/steels-science/](http://www.dierk-raabe.com/steels-science/).